tvst

Article

Quantification of Increased Corneal Subbasal Nerve Tortuosity in Dry Eye Disease and Its Correlation With Clinical Parameters

Baikai Ma[1,*], Jianyang Xie[2,*], Tingting Yang[1,5,*], Pan Su[2], Rongjun Liu[1], Tong Sun[1], Yifan Zhou[1], Haiwei Wang[1,3], Xue Feng[1,4], Siyi Ma[1], Yitian Zhao[2], and Hong Qi[1]

[1] Department of Ophthalmology, Peking University Third Hospital, Beijing Key Laboratory of Restoration of Damaged Ocular Nerve, Beijing, China
[2] Cixi Institute of BioMedical Engineering, Ningbo Institute of Materials Technology and Engineering, Chinese Academy of Sciences, Ningbo, China
[3] Department of Ophthalmology, Fuxing Hospital, Capital Medical University, Beijing, China
[4] Department of Ophthalmology, Beijing Moslem People's Hospital, Beijing, China
[5] Institute of Medical Technology, Peking University Health Science Center, Beijing, China

Correspondence: Hong Qi, Department of Ophthalmology, Peking University Third Hospital, Beijing Key Laboratory of Restoration of Damaged Ocular Nerve, 49 North Garden Rd, Haidian District, Beijing 100191, China.
e-mail: doctorqihong@163.com

Received: November 10, 2020
Accepted: April 8, 2021
Published: May 20, 2021

Keywords: dry eye disease; corneal subbasal nerve; tortuosity; aggregated measure

Citation: Ma B, Xie J, Yang T, Su P, Liu R, Sun T, Zhou Y, Wang H, Feng X, Ma S, Zhao Y, Qi H. Quantification of increased corneal subbasal nerve tortuosity in dry eye disease and its correlation with clinical parameters. Transl Vis Sci Technol. 2021;10(6):26, https://doi.org/10.1167/tvst.10.6.26

Purpose: This study quantified corneal subbasal nerve tortuosity in dry eye disease (DED) and investigated its correlation with clinical parameters by proposing an aggregated measure of tortuosity (Tagg).

Methods: The sample consisted of 26 eyes of patients with DED and 23 eyes of healthy volunteers, which represented separately the dry eye group and the control group. Clinical evaluation of DED and in vivo confocal microscopy analysis of the central cornea were performed. Tagg incorporated six metrics of tortuosity. Corneal subbasal nerve images of subjects and a validation data set were analyzed using Tagg. Spearman's rank correlation was performed on Tagg and clinical parameters.

Results: Tagg was validated using 1501 corneal nerve images. Tagg was higher in patients with DED than in healthy volunteers ($P < 0.001$). Tagg was positively correlated with the ocular surface disease index ($r = 0.418$, $P = 0.003$) and negatively correlated with tear breakup time ($r = -0.398$, $P = 0.007$). There was no correlation between Tagg and visual analog scale scores, corneal fluorescein staining scores, or the Schirmer I test.

Conclusions: Tagg was validated for quantification of corneal subbasal nerve tortuosity and was higher in patients with DED than in healthy volunteers. A higher Tagg may be linked to ocular discomfort, visual function disturbance, and tear film instability.

Translational Relevance: Corneal subbasal nerve tortuosity is a potential biomarker for corneal neurobiology in DED.

Introduction

Dry eye disease (DED) has been defined as "a multifactorial disease of the ocular surface characterized by a loss of homeostasis of the tear film, and accompanied by ocular symptoms."[1] Overall prevalence of DED, based on symptoms and signs, ranges from 8.7% to 30.1%[2] and is on the increase because of rapidly aging populations and the ubiquitous use of visual displays.[3,4] This results in a decreased vision-related quality of life and a large economic burden to society.[5]

It has been established that corneal nerve structure and function are closely linked to DED,[6–8] and the Tear Film & Ocular Surface Society acknowledged the etiological role of neurosensory abnormalities in DED during the Dry Eye Workshop II (DEWS II).[1] The corneal subbasal nerve plexus, located between

Bowman's layer and the basal epithelial layer, constitutes the densest layer of human corneal innervation.[9] It is readily visualized by in vivo confocal microscopy (IVCM), so that IVCM has become the method of choice to analyze corneal nerves. In a recent review of the use of IVCM in DED, corneal subbasal nerves were implicated in the pathogenesis of DED.[10] Except for density and beadings, corneal subbasal nerve tortuosity in DED has raised great interest in recent years. Several studies have reported increased corneal subbasal nerve tortuosity in primary Sjögren syndrome-related DED, non-Sjögren syndrome-related DED, and symptomatic contact lens-related DED.[11–13]

However, research on tortuosity of corneal nerves is challenging due to its vague definition. Current methods to assess corneal nerve tortuosity were mostly subjective with poor reproducibility across studies.[14,15] Therefore, several teams have raised objective measures of quantifying corneal nerve tortuosity.[16–18] We previously applied single objective metrics, such as arc length over chord length ratio (LC), to demonstrate that corneal subbasal nerve tortuosity was higher in patients with DED than in non-DED volunteers.[19] However, tortuosity is a multifaceted feature that cannot be accurately described with a single measure.[17] Hence, an aggregated measure is needed to more accurately determine corneal subbasal nerve tortuosity and its clinical significance in DED. In this study, we quantified corneal subbasal nerve tortuosity in DED and further investigated its correlation with clinical parameters, using an aggregated measure of tortuosity (Tagg).

Methods

Design and Setting

This cross-sectional study was conducted from January 2018 to July 2019 at the Department of Ophthalmology, Peking University Third Hospital. All subjects gave their informed consent for inclusion in the study. The study was performed in accordance with the Declaration of Helsinki, and the protocol was approved by the Institutional Review Board (Peking University Third Hospital, IRB00006761-M2017354).

Clinical Subjects

Patients with DED (DE group) and healthy volunteers without DED (control group) were recruited. We diagnosed DED according to the DEWS II criteria: (1) the Ocular Surface Disease Index (OSDI) $\geq$13; (2) tear breakup time (TBUT) $<$ 10 seconds; or $>$ five spots of corneal fluorescein staining (CFS).[20] Healthy volunteers were asymptomatic, with a clear, healthy cornea and stable tear film. Exclusion criteria for both groups were: a history of ocular surgery; contact lenses worn within one month prior to recruitment; meibomian gland dysfunction over stage 3;[21] blink disorders; topical medication applications within two weeks prior to recruitment; DED-related systemic diseases such as Sjögren syndrome or diabetes.[22]

Ocular Surface Evaluation

Evaluations were performed sequentially from the least to the most invasive, based on our previous study.[23] In brief, patients completed an OSDI questionnaire and a visual analog scale (VAS; from 0 [no pain] to 10 [very severe pain]). Thereafter, a Schirmer I test was performed without anesthesia, and the length of wet filter paper (mm) was recorded. Five minutes later, TBUT was assessed by gently touching the lower palpebral conjunctiva with a wet fluorescein strip. The CFS score was graded from 0 to 15. Corneal sensitivity (Cochet-Bonnet esthesiometry [C-BE]) was evaluated using a Cochet-Bonnet esthesiometer (Luneau Technology Operations SAS, Pont-de-l'Arche, France), with the filament extended to 6 cm, and reduced to 0 cm in 0.5-cm steps. The maximum length was recorded when subject perceived touch. For each subject, measurements were obtained from right eye.

Image Acquisition

After ocular surface evaluation, IVCM (Heidelberg Retina Tomograph 3/Rostock Cornea Module; Heidelberg Engineering GmbH, Heidelberg, Germany) was conducted to obtain corneal subbasal nerve images. After topical anesthesia, 0.2% carboxypolymethylene gel was applied to eyes and the outside tip of the cap to improve optical coupling. Images were acquired at a distance of 40–60 µm from the anterior surface of the central cornea. Images were 384 $\times$ 384 pixels, covering an area of 400 $\times$ 400 µm. Five images of each eye were obtained for tortuosity analysis.

Data Set for Validation

A data set of corneal nerve images was randomly chosen from the IVCM library of Peking University Third Hospital to validate Tagg. Images were chosen irrespective of disease, age, or corneal location. However, images containing abnormal structures such as dendritic cells and obvious neuromas were excluded to avoid biases in automatic segmentation of nerves. All images for validation were classified into four tortuosity subsets, from Grade I to Grade IV, according

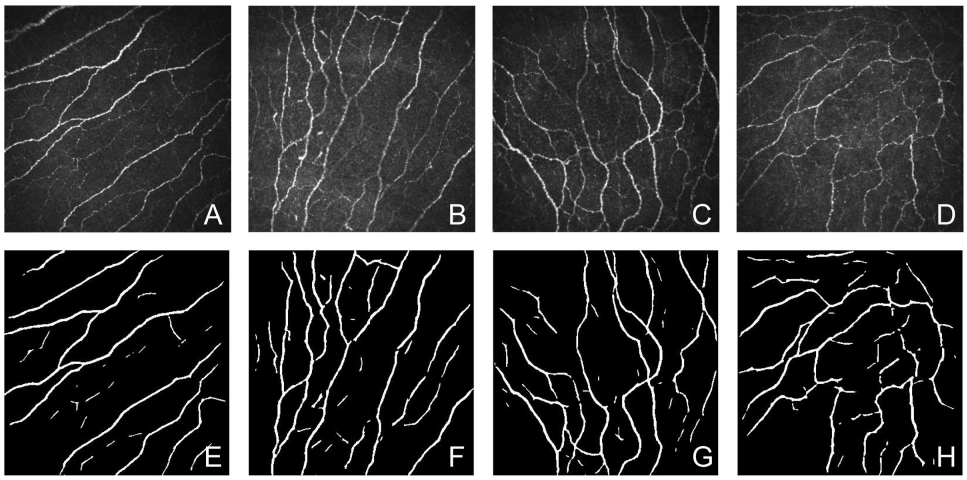

Figure 1. Representative raw corneal nerve images of Grade I, II, III, and IV tortuosity, based on the method of Oliveira-Soto and Efron[24] (**A, B, C,** and **D**, respectively), and corresponding segmented nerves (**E, F, G**, and **H**, respectively). Grade I: nerve fibers are straight or slightly tortuous. Grade II: nerve fibers are moderately tortuous with minor changes in direction. Grade III: nerve fibers are quite tortuous with obvious changes in direction. Grade IV: nerve fibers are severely tortuous with abrupt and frequent changes in direction.

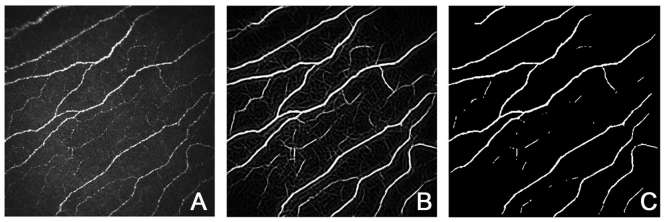

Figure 2. Representative original corneal nerve image (**A**), local phase (LP)–based enhancement (**B**), and IPACHI-based segmentation (**C**).

to the method of Oliveira-Soto and Efron.[24] Grading was performed independently by two experienced ophthalmologists. Representative images of Grade I to Grade IV are depicted in Figures 1A–D.

Automatic Nerve Segmentation

The method proposed by Zhao et al.[25] was applied to automatically segment nerves of subjects and those of validation images. This method adopts an infinite perimeter active contour with hybrid region information (IPACHI) model on the basis of local phase (LP) enhancement and intensity information. The LP based enhancement map is used for its superiority in preserving nerve edges. The given image intensity information helps to exclude some potential outliers in the image and guarantees a correct feature's segmentation. After enhancement, segmentation was performed by the IPACHI model. The representative figures of original image, enhancement and segmentation are listed in Figures 2A–C. We previously achieved satisfactory interobserver and intraobserver agreements via manual annotation,[26] as well as excellent comparability between automatic segmentation and expert annotation.[27] Representative segments of raw images from Grade I to Grade IV are depicted in Figures 1E–H.

Single and Aggregated Tortuosity Measures

After nerve segmentation, single and aggregated tortuosity measures were calculated. Single tortuosity metrics were divided into three categories: length-based, curvature-based, and mixed tortuosity.[28] However, tortuosity is a multifaceted feature so that using only one metric to quantify nerve tortuosity is one-sided and biased. To produce a more robust overall assessment, we calculated Tagg, using multiple measures simultaneously. We selected six metrics for aggregation on the basis of our prior study.[19] The details of single measures are described in Table 1.

In this study, a data-driven aggregation operator, kNN-DOWA,[29] was used to perform reliability-weighted averaging of multiple tortuosity measures based on first third of the nerve fibers sorted by nerve length.[30] This method was used to estimate the reliability of a tortuosity measurement by measuring the distance from that value to its k nearest neighbors; a smaller value indicated a higher reliability. For example, given a nerve fiber segment and its tortuosity measurement LC, the weight of LC was inversely proportional to the distance between LC and its k nearest neighbors among curvature maximum (Cur_max), total curvature (TC), total squared

Table 1. Detailed Information of Single Measures of Tortuosity

Categories of Tortuosity	Tortuosity Measures[28]
Length-based tortuosity	Arc length over chord length ratio
Curvature-based tortuosity	Curvature maximum
	Total curvature
	Total squared curvature
	Absolute direction angle change
Mixed tortuosity	Inflection count metric

curvature (TSC), absolute direction angle change (DCI), and infection count metric (ICM). Because the value ranges of the selected tortuosity measures were different, all values were normalized to a value between 0 and 1 before aggregation. The number of nearest neighbors in kNN-DOWA was set to three, with the aim of using more than half of the available tortuosity values to estimate the reliability of the underlying value.

Statistical Analysis

Summary data were presented as mean (standard deviation, SD) for continuous variables and median (first and third quartiles, Q1 and Q3) for rank variables. Independent-samples *t*-test, Mann-Whitney U test, or one-way analysis of variance was applied where appropriate. Spearman's rank correlation was used to explore the relationship between Tagg and clinical parameters. Values of $P < 0.05$ were considered statistically significant. Statistical analyses were performed with IBM SPSS Statistics for Windows (Version 24.0; IBM Corp., Armonk, NY, USA).

Results

Demographic and Clinical Characteristics of Subjects

This study included 23 eyes of 23 healthy volunteers (control group) and 26 eyes of 26 patients with DED (DE group). Demographic data and clinical characteristics of these groups are presented in Table 2. Age and sex of the two groups were matched ($P = 0.077$ and $P = 0.622$, respectively). Compared with the control group, the DE group had higher OSDI and CFS scores (both $P < 0.001$), but a shorter TBUT ($P < 0.001$). However, there was no difference in the Schirmer I test value between the two groups ($P = 0.454$). Compared with the control group, the DE group had higher VAS scores ($P < 0.001$) but a similar C-BE value ($P = 0.362$).

Validation of Tagg in Evaluating Corneal Nerve Tortuosity

We finally selected 1501 images from the IVCM library for the validation data set, including Grade I

Table 2. Demographic Data and Clinical Characteristics of Subjects

Groups	Control Group	DE Group	$\chi^2/t/Z$ Value	*P* Value
Patients/eyes, n/n	23/23	26/26		
Sex (M/F), n/n	4/19	6/20	0.243	0.622*
Age (years), mean (SD)	61.78 (9.17)	54.58 (17.68)	1.82	0.077†
OSDI, mean (SD)	8.84 (4.92)	29.85 (14.36)	−6.992	<0.001†
VAS score median (Q1, Q3)	0 (0, 0)	1 (0, 3)	−3.853	<0.001‡
TBUT(s), mean (SD)	8.09 (3.32)	4.96 (1.82)	3.945	<0.001†
CFS score Median (Q1, Q3)	0 (0, 2.25)	3 (1, 6.25)	−3.413	<0.001‡
Schirmer I test(mm) mean (SD)	9.59 (6.36)	11.27 (8.63)	−0.755	0.454†
C-BE (cm) median (Q1, Q3)	6 (6, 6)	6 (5, 88, 6)	−0.912	0.362‡

*χ^2 test.
†Independent-samples *t* test.
‡Mann-Whitney U test.
DE, dry eye.

Table 3. Validation of Single and Aggregated Measures of Tortuosity in Corneal Nerve Images From Grade I to Grade IV

Grades	Grade I	Grade II	Grade III	Grade IV	*F*	*P*
LC (*10^{-3}), mean (SD)	43.71 (25.44)	55.89 (29.66)[‡]	69.23 (28.36)[‡,§]	94.02 (35.65)[‡,§,‖]	156.792	<0.001
Cur_max (*10^{-3}), mean (SD)	43.60 (10.87)	46.52 (9.01)[†]	49.82 (9.38)[‡,§]	54.93 (9.98)[‡,§,‖]	89.579	<0.001
TC (*10^{-3}), mean (SD)	10.44 (1.94)	11.85 (1.76)[‡]	12.92 (1.94)[‡,§]	14.52 (2.30)[‡,§,‖]	246.895	<0.001
TSC (*10^{-5}), mean (SD)	20.89 (8.89)	26.13 (8.13)[‡]	31.54 (10.78)[‡,§]	40.29 (13.23)[‡,§,‖]	206.890	<0.001
DCI (*10^{-6}), mean (SD)	17.23 (10.84)	22.35 (11.12)[‡]	28.88 (16.10)[‡,§]	38.90 (19.75)[‡,§,‖]	123.941	<0.001
ICM (*10^{-1}), mean (SD)	7.07 (4.06)	7.56 (4.22)[#]	8.96 (5.31)[‡,§]	11.20 (6.79)[‡,§,‖]	24.032	<0.001
Tagg (*10^{-2}), mean (SD)	14.95 (9.69)	19.82 (8.38)[‡]	25.37 (10.67)[‡,§]	34.06 (12.22)[‡,§,‖]	220.699	<0.001

One-way ANOVA was applied to test differences among the four groups. Tamhane's T2 test was applied as a post-hoc multiple comparisons test for pairwise comparison.

[†] $P < 0.01$, compared with Grade I.

[‡] $P < 0.001$, Compared with Grade I.

[§] $P < 0.001$, Compared with Grade II.

[‖] $P < 0.001$, Compared with Grade III.

[#] $P \geq 0.05$, Compared with Grade III.

Table 4. Corneal Subbasal Nerve Tortuosity in the Control Group and the DE Group

Groups	Control Group	DE Group	*t*	*P*
Number of images	115	130		
LC (*10^{-3}), mean (SD)	42.24 (15.06)	53.29 (32.04)	−3.761	<0.001
Cur_max (*10^{-3}), mean (SD)	42.21 (7.88)	46.10 (9.23)	−3.718	<0.001
TC (*10^{-3}), mean (SD)	11.36 (1.61)	12.27 (2.34)	−3.816	<0.001
TSC (*10^{-5}), mean (SD)	25.48 (7.33)	30.15 (11.49)	−4.093	<0.001
DCI (*10^{-6}), mean (SD)	22.12 (9.69)	28.87 (16.71)	−4.19	<0.001
ICM (*10^{-1}), mean (SD)	5.56 (3.71)	6.70 (5.29)	−2.079	0.039
Tagg (*10^{-2}), mean (SD)	19.75 (8.33)	25.46 (12.23)	−4.61	<0.001

Independent-samples *t*-tests were applied to test differences between the two groups.

(214 images, 14.3%), Grade II (461 images, 30.7%), Grade III (364 images, 24.3%), and Grade IV (462 images, 30.7%) tortuosity. Single tortuosity measures and Tagg of corneal nerve images in these subsets are indicated in Table 3. LC, Cur_max, TC, TSC, and DCI increased from Grade I to Grade IV ($P < 0.01$ for all pairwise comparisons). Meanwhile, although no statistically significant difference in ICM was observed between Grade I and Grade II ($P = 0.634$), ICM increased from Grade II to Grade IV ($P < 0.001$ for all pairwise comparisons among Grade II, Grade III and Grade IV). These results indicated that the six single metrics were effective in quantifying corneal nerve tortuosity.

We normalized and aggregated these single metrics into Tagg. We revealed that Tagg increased from Grade I to Grade IV ($P < 0.001$ for all pairwise comparisons), with a high *F* value (220.699), comparable to that of TC (246.895) and TSC (206.890).

Corneal Subbasal Nerve Tortuosity in Patients With DED

We analyzed 115 corneal subbasal nerve images in the control group (24, 84, 7, 0 images from Grade I to Grade IV, respectively) and 130 images in the DE group (7, 66, 50, 7 images from Grade I to Grade IV, respectively) using single tortuosity metrics and Tagg (Table 4). All six values of the DE group were higher than those of the control group (ICM, $P < 0.05$; all other metrics, $P < 0.001$). However, there were discordances when comparing values of some of these single metrics to those of the validation group. For example, the LC and Cur_max values of the control group were

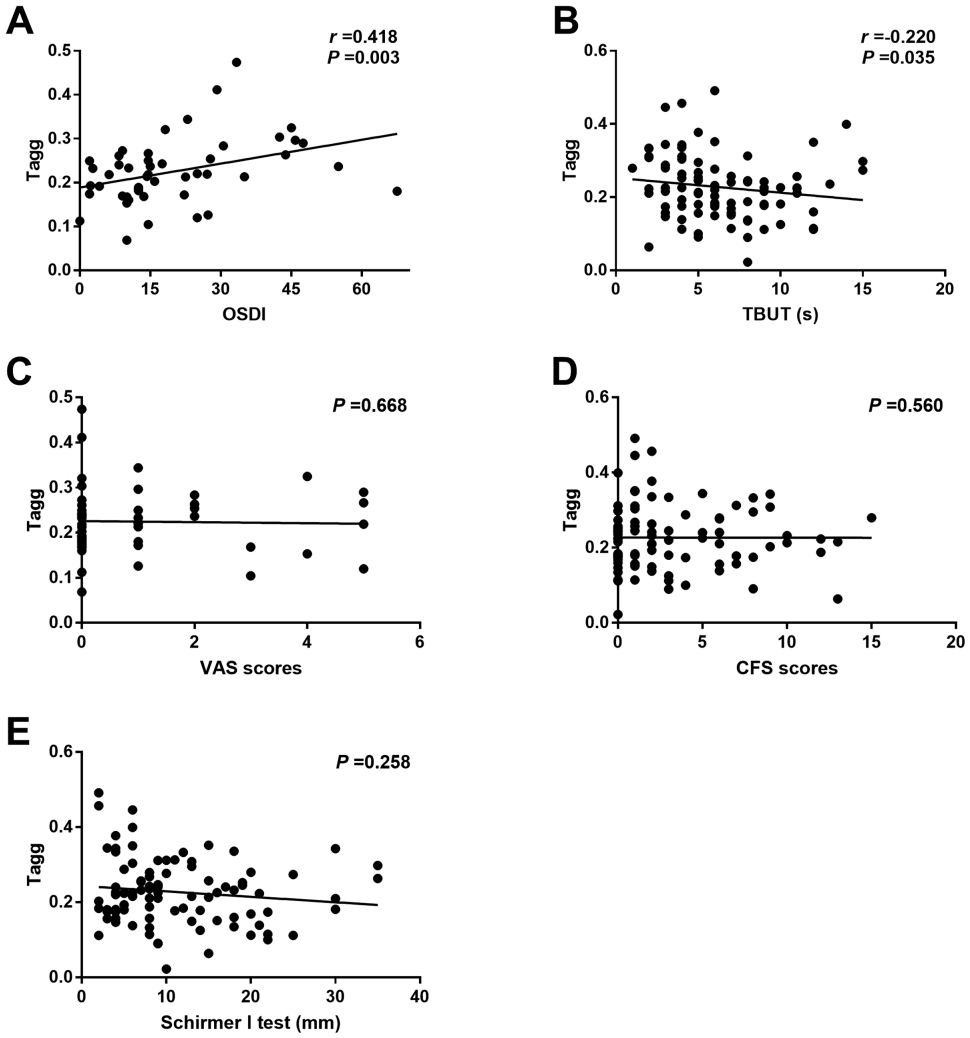

Figure 3. Correlations of the aggregated measure of corneal subbasal nerve tortuosity (Tagg) and clinical parameters of DED. Spearman's rank correlation indicated that Tagg positively correlated with the OSDI (**A**) and negatively correlated with TBUT (**B**). Tagg did not correlate with VAS scores (**C**), CFS scores (**D**), or the Schirmer I test (**E**). CFS, corneal fluorescein staining; DED, dry eye disease; OSDI, ocular surface disease index; TBUT, tear breakup time; VAS, visual analog score.

lower than those of Grade I images in the validation data set; values of the same indicators of the DE group were between those of Grade I and Grade II images. However, TC, TSC, and DCI values of the control group were between those of Grade I and Grade II images; values of the same three metrics of the DE group were between those of Grade II and Grade III images. ICM values of both groups were lower than those of Grade I images. The Tagg value of the DE group, which was similar to that of Grade III images, was higher than that of the control group, which was similar to that of Grade II images ($P < 0.001$).

Corneal Subbasal Nerve Tortuosity Correlation Analysis

Tagg was positively correlated with the OSDI ($P < 0.01$, $r = 0.418$) (Fig. 3A) and negatively correlated with TBUT ($P < 0.001$, $r = -0.398$) (Fig. 3B). However, no correlations were observed between Tagg and VAS scores, CFS scores, or Schirmer I test ($P = 0.67$, 0.47, and 0.59, respectively) (Figs. 3C–E).

Discussion

Morphological alterations of corneal subbasal nerves are objective parameters for evaluating ocular surface neurobiology in DED. There have been conflicting reports regarding nerve density in DED, including a decrease,[11,12] no change,[31,32] and an increase.[33] Reports of subbasal nerve tortuosity have more consistently revealed an increase in DED.[11,12,32–34] However, most of these studies used subjective grading systems, not quantifying tortuosity,

thereby decreasing the reproducibility and clinical significance of their results. Therefore, in this study, we quantified corneal subbasal nerve tortuosity in DED using Tagg, an objective and aggregated measure of tortuosity, and evaluated its correlation with clinical parameters of DED.

Scarpa et al.[16] and our group[19] previously proposed objective metrics of corneal nerve tortuosity. Lagali et al.[35] and Guimarães et al.[17] suggested that tortuosity was a multifaceted problem which needed overall assessment. Guimarães et al.[17] sorted images on the basis of short-range and long-range tortuosity and built two mixed models for the two image sets. Included tortuosity metrics of the two mixed models were different so that their method required manual classification of corneal nerve images, which is inconvenient. Here, for the first time, to our knowledge, we proposed and validated an aggregated and universal measure to quantify corneal nerve tortuosity. We previously explored reliability-guided aggregation and achieved Spearman's correlation coefficients of 0.7558 and 0.8279 for automatic and manual nerve segmentation, respectively, using 30 images.[36] In the present study, we incorporated six tortuosity metrics from three tortuosity categories into Tagg. We validated Tagg using a library of 1501 images according to four grades of tortuosity. Tagg was effective in differentiating images of different grades ($P < 0.001$ between any two grades), indicating that it is a promising metric to quantify corneal nerve tortuosity in healthy individuals and patients with DED. Although Tagg showed a lower F value (220.699) than that of TC (246.895), Tagg represents more features of nerve tortuosity and is more applicable than TC.

In our study, patients with DED experienced discomfort and visual function disturbance and exhibited corneal epithelial damage and unstable tear films. After validation, we applied single metrics and Tagg to demonstrate that corneal subbasal nerve tortuosity in patients with DED was higher than that in healthy controls. Moreover, Tagg has an advantage over single metrics, because there were discordances among the latter. For instance, LC, Cur_max, and ICM values of healthy volunteers were lower than those of Grade I images in the validation data set, whereas TC, TSC, and DCI values of healthy volunteers were between those of Grade I and Grade II images. These discordances reflected the different features that the metrics represent.

To further investigate the clinical significance of corneal subbasal nerve tortuosity in DED, we performed correlation analyses between Tagg and clinical parameters of DED. Tagg was positively correlated with OSDI and negatively correlated with TBUT, which indicated that corneal nerves might be more tortuous with increasing frequencies of ocular discomforts and visual function disturbance, as well as severer tear film instability in DED. Contrary to these results, a recent study discovered no correlation between corneal subbasal nerve tortuosity and the OSDI,[37] which was perhaps affected by the subjective grading system of tortuosity used. Our results suggest that corneal subbasal nerve tortuosity may be a morphological biomarker for corneal neurobiology in DED. As for the mechanism of tortuous corneal nerves in DED, it was hypothesized to be due to the release of nerve growth factors in response to the inflammatory factors.[38] In addition, because of unsound correlation between corneal morphology and functions,[38] the detailed contribution of tortuous subbasal corneal nerves to dysregulated nerve functions such as nociceptive neuropeptide secretion and pathogenesis of DED still remain to be answered.

Corneal sensitivity for blink and for perception of touch are widely applied to assess corneal sensation. Several studies demonstrated a reduction of corneal sensitivity for blink in DED,[12,39] but another report showed an increased corneal sensitivity for blink in DED.[40] Therefore we applied corneal sensitivity for perception of touch between patients with DED and healthy volunteers and found no difference. Kaido et al.[40] similarly reported that sensitivity for perception of touch was about the same between eyes with DED symptoms and eyes without. The reason may be that the sensitivity for perception of touch need minimal mechanical stimulus and will be impaired only if lots of corneal nerves are damaged. Neuropathic ocular pain in DED can be triggered by ocular surface inflammation and neurotransmitter release, as well as by abnormal morphological changes of corneal nerves.[40,41] In our study, patients with DED experienced more severe neuropathic ocular pain than healthy volunteers did, although we observed no correlation between Tagg and VAS score. This may be explained by the typically milder injuries of cornea nerves in DED than in refractive surgery, and subbasal nerve tortuosity may not be associated with nociceptors.

In this study, no correlation was observed between Tagg and the Schirmer I test. In contrast, Cardigos et al.[11] reported that corneal subbasal nerve tortuosity was negatively correlated with the Schirmer I test. However, they recruited Sjögren syndrome patients, which we excluded from our study. In their study, the Schirmer I test value in the non-Sjögren syndrome group (mean [SD]) was much lower than that of the control group (7.1 [6.3] vs. 22.3 [8.3]). In our study, there was no statistically significant difference in Schirmer I test value between the DE group and the

control group (10.86 [7.03] vs. 11.79 [8.31]). Notably, short-TBUT-type DED is more prevalent than other DED types in Asia, and many of these patients tend to have a normal Schirmer I test value.[42,43] In addition, both Cardigos et al.[11] and we observed no correlation between tortuosity and CFS scores. The reason could be that disruption of tight junctions, accountable for positive CFS, occurred in the epithelium on the superior surface of the cornea, but not in the subbasal layer, where nerve trunks are located.

The main limitation of this study is that we did not assess tear composition for inflammatory agents and neurotransmitters or other features of corneal subbasal nerves. We would like to investigate the role of morphological changes of corneal nerves in the pathogenesis of DED, and its link with tear film instability and inflammation, in future research. Another limitation is that analysis of the whole corneal nerve plexus is not yet possible. A way to match the same corneal location in images of different subjects or times needs to be developed. In addition, we excluded IVCM images with dendritic cells and obvious neuromas because we found that dendritic cells will be co-segmented with nerves, thus decreasing corneal nerve tortuosity (Supplementary Figure). The segmentation algorithm should be optimized in future study to eliminate the influence of abnormal features, which will facilitate analysis of corneal nerve, including but not limited to Tagg.

In conclusion, we quantified the increased corneal subbasal nerve tortuosity in DED using a universally aggregated measure, Tagg. Moreover, we elucidated that Tagg was moderately correlated with the OSDI and TBUT, which suggested that increased corneal subbasal nerve tortuosity was linked to frequencies of ocular discomfort, visual function disturbance, and tear film instability in DED. Corneal subbasal nerve tortuosity may be a biomarker for corneal neurobiology in DED.

Acknowledgments

Supported by the National Natural Science Foundation of China (81974128, 81570813 and 61906181), the Capital Health Research and Development of Special (2020-2-4097), and the Zhejiang Provincial Natural Science Foundation of China (LQ20F030002).

Disclosure: **B. Ma,** None; **J. Xie,** None; **T. Yang,** None; **P. Su,** None; **R. Liu,** None; **T. Sun,** None; **Y. Zhou,** None; **H. Wang,** None; **X. Feng,** None; **S. Ma,** None; **Y. Zhao,** None; **H. Qi,** None

[*] BM, JX and TY contributed equally to this work.

References

1. Craig JP, Nichols KK, Akpek EK, et al. TFOS DEWS II Definition and Classification Report. *Ocul Surf*. 2017;15:276–283.
2. Stapleton F, Alves M, Bunya VY, et al. TFOS DEWS II Epidemiology Report. *Ocul Surf.* 2017;15:334–365.
3. Ahn JM, Lee SH, Rim TH, et al. Prevalence of and risk factors associated with dry eye: the Korea National Health and Nutrition Examination Survey 2010-2011. *Am J Ophthalmol*. 2014;158:1205–1214.e1207.
4. Kaido M, Kawashima M, Yokoi N, et al. Advanced dry eye screening for visual display terminal workers using functional visual acuity measurement: the Moriguchi study. *Br J Ophthalmol*. 2015;99:1488–1492.
5. Clayton JA. Dry Eye. *N Engl J Med*. 2018;378:2212–2223.
6. Galor A, Levitt RC, Felix ER, Martin ER, Sarantopoulos CD. Neuropathic ocular pain: an important yet underevaluated feature of dry eye. *Eye (Lond)*. 2015;29:301–312.
7. Lambiase A, Micera A, Sacchetti M, Cortes M, Mantelli F, Bonini S. Alterations of tear neuromediators in dry eye disease. *Arch Ophthalmol*. 2011;129:981–986.
8. Belmonte C, Nichols JJ, Cox SM, et al. TFOS DEWS II pain and sensation report. *Ocul Surf*. 2017;15:404–437.
9. Müller LJ, Marfurt CF, Kruse F, Tervo TM. Corneal nerves: structure, contents and function. *Exp Eye Res*. 2003;76:521–542.
10. Matsumoto Y, Ibrahim OMA. Application of In Vivo Confocal Microscopy in Dry Eye Disease. *Invest Ophthalmol Vis Sci*. 2018;59:DES41–DES47.
11. Cardigos J, Barcelos F, Carvalho H, et al. Tear meniscus and corneal sub-basal nerve plexus assessment in primary Sjogren syndrome and sicca syndrome patients. *Cornea*. 2019;38:221–228.
12. Levy O, Labbé A, Borderie V, et al. Increased corneal sub-basal nerve density in patients with Sjögren syndrome treated with topical cyclosporine A. *Clin Exp Ophthalmol*. 2017;45:455–463.
13. Labbe A, Liang Q, Wang Z, et al. Corneal nerve structure and function in patients with non-Sjogren dry eye: clinical correlations. *Invest Ophthalmol Vis Sci*. 2013;54:5144–5150.
14. Hertz P, Bril V, Orszag A, et al. Reproducibility of in vivo corneal confocal microscopy as a

novel screening test for early diabetic sensorimotor polyneuropathy. *Diabet Med*. 2011;28:1253–1260.
15. Cruzat A, Qazi Y, Hamrah P. In vivo confocal microscopy of corneal nerves in health and disease. *Ocul Surf*. 2017;15:15–47.
16. Scarpa F, Zheng X, Ohashi Y, Ruggeri A. Automatic evaluation of corneal nerve tortuosity in images from in vivo confocal microscopy. *Invest Ophthalmol Vis Sci*. 2011;52:6404–6408.
17. Guimarães P, Wigdahl J, Ruggeri A. Automatic estimation of corneal nerves focused tortuosities. *Conf Proc IEEE Eng Med Biol Soc*. 2016;2016:1332–1335.
18. Kallinikos P, Berhanu M, O'Donnell C, Boulton AJ, Efron N, Malik RA. Corneal nerve tortuosity in diabetic patients with neuropathy. *Invest Ophthalmol Vis Sci*. 2004;45:418–422.
19. Ma B, Zhao K, Ma S, et al. Objective analysis of corneal subbasal nerve tortuosity and its changes in patients with dry eye and diabetes. *Chinese J Exp Ophthalmol*. 2019;37:638–644.
20. Wolffsohn JS, Arita R, Chalmers R, et al. TFOS DEWS II Diagnostic Methodology report. *Ocul Surf*. 2017;15:539–574.
21. Arita R, Itoh K, Inoue K, Amano S. Noncontact infrared meibography to document age-related changes of the meibomian glands in a normal population. *Ophthalmology*. 2008;115:911–915.
22. Mansoor H, Tan HC, Lin MT, Mehta JS, Liu YC. Diabetic corneal neuropathy. *J Clin Med*. 2020;9:3956.
23. Liu R, Ma B, Gao Y, Ma B, Liu Y, Qi H. Tear inflammatory cytokines analysis and clinical correlations in diabetes and nondiabetes with dry eye. *Am J Ophthalmol*. 2019;200:10–15.
24. Oliveira-Soto L, Efron N. Morphology of corneal nerves using confocal microscopy. *Cornea*. 2001;20:374–384.
25. Zhao Y, Rada L, Chen K, Harding SP, Zheng Y. Automated vessel segmentation using infinite perimeter active contour model with hybrid region information with application to retinal images. *IEEE Trans Med Imaging*. 2015;34:1797–1807.
26. Borroni D, Beech M, Williams B, et al. Building a validated in vivo confocal microscopy (IVCM) dataset for the study of corneal nerves. *Invest Ophthalmol Vis Sci*. 2018;59.
27. Qi H, Borroni D, Liu RJ, et al. Automated detection of corneal nerves using deep learning. *Invest Ophthalmol Vis Sci*. 2018;59.
28. Abdalla M, Hunter A, Al-Diri B. Quantifying retinal blood vessels' tortuosity. In *Science and Information Conference*. London: IEEE; 2015:687–693.
29. Boongoen T, Shen Q. Nearest-neighbor guided evaluation of data reliability and its applications. *IEEE Trans Syst Man Cybern B Cybern*. 2010;40:1622–1633.
30. Su P, Chen T, Xie J, et al. Corneal nerve tortuosity grading via ordered weighted averaging-based feature extraction. *Med Phys*. 2020;47:4983–4996.
31. Hosal BM, Ornek N, Zilelioglu G, Elhan AH. Morphology of corneal nerves and corneal sensation in dry eye: a preliminary study. *Eye (Lond)*. 2005;19:1276–1279.
32. Dogan AS, Gurdal C, Arslan N. Corneal confocal microscopy and dry eye findings in contact lens discomfort patients. *Cont Lens Anterior Eye*. 2018;41:101–104.
33. Zhang M, Chen J, Luo L, Xiao Q, Sun M, Liu Z. Altered corneal nerves in aqueous tear deficiency viewed by in vivo confocal microscopy. *Cornea*. 2005;24:818–824.
34. Villani E, Magnani F, Viola F, et al. In vivo confocal evaluation of the ocular surface morphofunctional unit in dry eye. *Optom Vis Sci*. 2013;90:576–586.
35. Lagali N, Poletti E, Patel DV, et al. Focused tortuosity definitions based on expert clinical assessment of corneal subbasal nerves. *Invest Ophthalmol Vis Sci*. 2015;56:5102–5109.
36. Pan S, Yitian Z, Tianhua C, et al. Exploiting reliability-guided aggregation for the assessment of curvilinear structure tortuosity. In *Medical Image Computing and Computer Assisted Intervention - MICCAI 2019 22nd International Conference Proceedings Lecture Notes in Computer Science (LNCS 11767)*. Cham: Springer; 2019:12–20.
37. Liu Y, Chou Y, Dong X, et al. Corneal subbasal nerve analysis using in vivo confocal microscopy in patients with dry eye: analysis and clinical correlations. *Cornea*. 2019;38:1253–1258.
38. Al-Aqaba MA, Dhillon VK, Mohammed I, Said DG, Dua HS. Corneal nerves in health and disease. *Prog Retin Eye Res*. 2019;73:100762.
39. Nepp J, Wirth M. Fluctuations of corneal sensitivity in dry eye syndromes—a longitudinal pilot study. *Cornea*. 2015;34:1221–1226.
40. Kaido M, Kawashima M, Ishida R, Tsubota K. Relationship of corneal pain sensitivity with dry eye symptoms in dry eye with short tear break-up time. *Invest Ophthalmol Vis Sci*. 2016;57:914–919.
41. Khamar P, Nair AP, Shetty R, et al. Dysregulated tear fluid nociception-associated factors, corneal dendritic cell density, and vitamin D levels in evaporative dry eye. *Invest Ophthalmol Vis Sci*. 2019;60:2532–2542.

42. Tsubota K, Yokoi N, Shimazaki J, et al. New perspectives on dry eye definition and diagnosis: a consensus report by the Asia Dry Eye Society. *Ocul Surf*. 2017;15:65–76.

43. Uchino M, Yokoi N, Uchino Y, et al. Prevalence of dry eye disease and its risk factors in visual display terminal users: the Osaka Study. *Am J Ophthalmol*. 2013;156:759–766.